Cancer Cell
Article

Increased Radioresistance and Accelerated B Cell Lymphomas in Mice with Mdmx Mutations that Prevent Modifications by DNA-Damage-Activated Kinases

Yunyuan V. Wang,[1] Mathias Leblanc,[1] Mark Wade,[1] Aart G. Jochemsen,[2] and Geoffrey M. Wahl[1,*]
[1]Gene Expression Laboratory, Salk Institute for Biological Studies, 10010 North Torrey Pines Road, La Jolla, CA 92037, USA
[2]Department of Molecular and Cell Biology, Leiden University Medical Center, 2300 ZA Leiden, the Netherlands
*Correspondence: wahl@salk.edu
DOI 10.1016/j.ccr.2009.05.008

SUMMARY

Mdmx is a critical negative regulator of the p53 pathway that is stoichiometrically limiting in some tissues. Posttranslational modification and degradation of Mdmx after DNA damage have been proposed to be essential for p53 activation. We tested this model in vivo, where critical stoichiometric relationships are preserved. We generated an Mdmx mutant mouse in which three conserved serines (S341, S367, S402) targeted by DNA-damage-activated kinases were replaced by alanines to investigate whether modifications of these residues are important for Mdmx degradation and p53 activation. The mutant mice were remarkably resistant to radiation, and very susceptible to Myc-induced lymphomagenesis. These data demonstrate that Mdmx downregulation is crucial for effective p53-mediated radiation responses and tumor suppression in vivo.

INTRODUCTION

The p53 tumor suppressor is a transcription factor that is activated by diverse conditions to induce or repress hundreds of protein- and miRNA-encoding genes (Toledo and Wahl, 2006). Its activation elicits responses ranging from reversible cell-cycle arrest to cellular senescence, cell death, blastocyst implantation, or cytokine induction to recruit the immune system (Riley et al., 2008). Its critical role in tumor suppression is evident from the tumor predisposition of mice and humans harboring germline p53 mutations (reviewed by Varley, 2003), and its mutation and loss of heterozygosity in 50% of human cancers (Vousden and Lu, 2002).

p53 function is also compromised in tumors encoding wild-type p53. This typically occurs by overexpression of either one of its two negative regulators, the oncoproteins Mdm2 and Mdmx (Marine and Jochemsen, 2005), or by loss of the tumor suppressor Arf (Eischen et al., 1999), which antagonizes Mdm2 (see below). Mice lacking either Mdm2 or Mdmx die during embryogenesis, and the embryonic lethality is rescued by *p53* deletion (Jones et al., 1995; Montes de Oca Luna et al., 1995; Parant et al., 2001; Migliorini et al., 2002). This demonstrates that Mdm2 and Mdmx serve nonredundant functions in p53 regulation. Both proteins bind to the same region in the p53 transcription activation domain, and inhibit p53-dependent transcription (reviewed by Marine et al., 2007). In addition, Mdm2 functions as a RING domain E3 ubiquitin ligase to mediate p53 degradation (Fang et al., 2000; Michael and Oren, 2003). Whereas Mdmx is also a RING domain protein that is highly homologous to Mdm2, it does not exhibit detectable E3 ligase activity (Stad et al., 2001). However, several studies have indicated that Mdmx can heterodimerize with Mdm2 and enhance or even rescue Mdm2 ligase activity (Uldrijan et al., 2007; Poyurovsky et al., 2007; Singh et al., 2007; Kawai et al., 2007). As with other RING domain E3 ligases such as BRCA1 and BARD1 (Christensen et al., 2007), it is likely that an Mdmx/Mdm2 heterodimer forms a more optimal interface to recruit one or more E2 ubiquitin transferases required to ubiquitylate p53 (Linke et al., 2008).

It has long been known that DNA double-strand breaks activate the ATM and Chk2 protein kinases to induce multiple

SIGNIFICANCE

p53 function is sensitive to the levels of its negative regulators, Mdm2 and Mdmx. Cell-culture studies have suggested the importance of posttranslational modifications in Mdm2 and Mdmx for p53 activation, but this has not been rigorously tested in vivo. This work shows that DNA damage and activated c-Myc both require phosphorylation of Mdmx in residues targeted by the damage kinases ATM and Chk2 for robust p53 activation. Preventing Mdmx posttranslational modification stabilizes this negative regulator, which mitigates p53 activation, and presumably enables c-Myc to drive tumor cells with defective genomes into cycle in vivo. The data also stress the relevance of Mdmx as a potential therapeutic target.

posttranslational modifications on p53 and Mdm2 (Shieh et al., 1997; Prives, 1998; Maya et al., 2001). In vitro data suggest that the N-terminal modifications of p53 near the Mdm2/Mdmx binding site may serve to reduce p53 interaction with these negative regulators, as well as enhancing association with the histone acetyltransferase coactivators that bind to the same region (Grossman et al., 1998). In mice, p53 posttranslational modifications serve the important function of fine-tuning p53 activity in different tissues (reviewed by Toledo and Wahl, 2006).

Another important contribution to p53 activation is the DNA-damage-induced, accelerated degradation of Mdm2 and Mdmx, which limits their ability to antagonize p53. We previously showed that phosphorylation of Mdm2 by DNA-damage-induced kinases accelerates Mdm2 autodegradation (Stommel and Wahl, 2004). Similarly, double-strand DNA breaks result in phosphorylation of human Mdmx at Ser342 and Ser367 by Chk2 (Okamoto et al., 2005; Chen et al., 2005; LeBron et al., 2006; Pereg et al., 2006) and Ser403 by ATM (Pereg et al., 2005), all of which are needed for efficient Mdmx degradation. These phosphorylations reduce binding of HAUSP, a ubiquitin-specific protease (Meulmeester et al., 2005), which appears to render Mdmx vulnerable to Mdm2-mediated ubiquitylation and proteasomal degradation (Kawai et al., 2003; de Graaf et al., 2003; Pan and Chen, 2003). Phosphorylations at Ser342 and Ser367 of Mdmx are also necessary for interaction with 14-3-3 proteins, which affect Mdmx nuclear accumulation and degradation (Okamoto et al., 2005; LeBron et al., 2006; Pereg et al., 2006; Jin et al., 2006), perhaps by serving as a steric barrier to limit HAUSP binding.

The molecular intermediates that transduce signals from activated oncogenes are beginning to be understood. As one example, c-Myc is a transcription factor that activates numerous genes including those involved in cell-cycle entry and progression, DNA replication, and metabolism (reviewed by Eilers and Eisenman, 2008). Although it is clear that c-Myc overexpression robustly activates p53, whether DNA damage is involved remains controversial (e.g., see Vafa et al., 2002; Maclean et al., 2003; Wade and Wahl, 2006). c-Myc overexpression results in induction of the INK4a/Arf tumor suppressor (Zindy et al., 1998). Arf binds to and inhibits Mdm2, which, as a consequence, leads to p53 activation and induction of p53-mediated downstream responses (Kamijo et al., 1998). The importance of the Arf-Mdm2-p53 pathway in Myc-induced tumorigenesis is evident in the *Eμ-Myc* lymphoma model where multiple copies of the *c-Myc* gene are overexpressed in the B cell lineage (Adams et al., 1985). Recently, an alternative mouse model (*iMyc*$^{E\mu}$) was generated by inserting a single *c-Myc* gene into the immunoglobulin heavy-chain enhancer (Eμ) (Park et al., 2005). This mimics the human t(8;14)(q24;q32) translocation that results in activation of c-Myc in human endemic Burkitt's lymphomas (Alitalo et al., 1987), and makes *iMyc*$^{E\mu}$ a better model for this disease. In both models, lymphomagenesis progresses when p53 function is abrogated by loss of *Arf*, overexpression of *Mdm2*, or mutation of *p53* (Eischen et al., 1999; Park et al., 2005). Consistent with these observations, deleting either the *p53* or *Arf* gene in *Eμ-Myc* mice accelerates the onset of lymphomas to the same extent (Eischen et al., 1999; Schmitt et al., 1999; Martins et al., 2006). In contrast, losing one copy of *Mdm2* increases lymphoma latency (Eischen et al., 2004; Terzian et al., 2007), whereas overexpressing *Mdm2* in *Eμ-Myc* mice decreases tumor latency (Wang et al., 2008). Recently, Terzian et al. (2007) showed that *Eμ-Myc;Mdmx*$^{+/-}$ mice also exhibited delayed lymphomagenesis, suggesting a role for Mdmx in Myc-induced tumorigenesis. However, the mechanism by which Mdmx contributes to Myc-induced tumorigenesis remains unclear.

Understanding the factors that control p53 activation requires that they be analyzed in physiologically relevant settings given the exquisite sensitivity of p53 to the levels of its negative regulators. We report the analysis of an Mdmx mutant mouse (hereafter *Mdmx*^{3SA}) designed to test the importance of three highly conserved serine residues targeted by the DNA-damage-activated kinases ATM (Ser402) and Chk2 (Ser341, Ser367) with regard to irradiation and c-Myc-driven tumorigenicity.

RESULTS

Generation of *Mdmx*^{3SA} Mice

We generated a mouse model in which the two highly conserved Chk2 sites at serines 341 and 367 and the ATM site at Ser402 of Mdmx were mutated to alanines to begin to evaluate the importance of Mdmx stability regulation in different tissues in vivo. The targeting construct (Figure 1A) was electroporated into the *Mdmx* locus of PrmCre embryonic stem cells, allowing for direct transfer of the edited allele upon mating of transmitting males (O'Gorman et al., 1997). Allele-specific PCR (see Figure S1 available online) and Southern blotting (Figure 1B) demonstrated that 5%–10% of all G418-resistant clones had undergone homologous recombination. Four independent homologous recombinant ES clones were injected into C57BL/6 blastocysts to produce *Mdmx*^{3SA} chimeras, and 80% (4/5) of male chimeras transmitted the mutant allele through the germline. *Mdmx*^{3SA} homozygotes were obtained by intercrossing heterozygous mutant mice and were generated at Mendelian ratios typical for the transmission of an autosomal allele lacking adverse developmental effects (Figure 1C). *Mdmx* transcripts expressed in thymus isolated from *Mdmx*^{3SA} mice were sequenced, and found to be wild-type for all codons except the three encoding the targeted mutations (Figures 1D and 1E). The genetic background for all studies is 50% 129/Sv and 50% C57BL/6. We have followed *Mdmx*^{3SA} homozygotes for more than 18 months, and have observed no obvious tumor predisposition or differences in vitality compared to WT mice (data not shown).

Mouse embryonic fibroblasts (MEFs) were isolated from embryonic day 13.5 (E13.5) to determine the biochemical consequences of DNA damage on cells expressing Mdmx^{WT} or Mdmx^{3SA}. Using an antibody specifically recognizing phospho-S367 of Mdmx, we detected robust accumulation of a doublet band in *Mdmx*^{WT} MEFs when cells were treated with the radiomimetic agent neocarzinostatin (NCS) plus proteasome inhibitors (PI) (Figure 2A). Note that a weak signal of phospho-S367 was detected in Mdmx^{WT} cells in the absence of exogenous damage (Figure 2A, lane 1), indicating that an intrinsic stress occurring during cell culture activates kinases that target this phosphorylation site in Mdmx. The slower-migrating band likely derives from the phosphorylation at S402 (Pereg et al., 2005), because an anti-phospho-S402 antibody only recognizes the slower-migrating band in NCS- plus PI-treated *Mdmx*^{WT} MEFs (Figure 2B). Importantly, the single Mdmx band observed in *Mdmx*^{3SA} MEFs did not

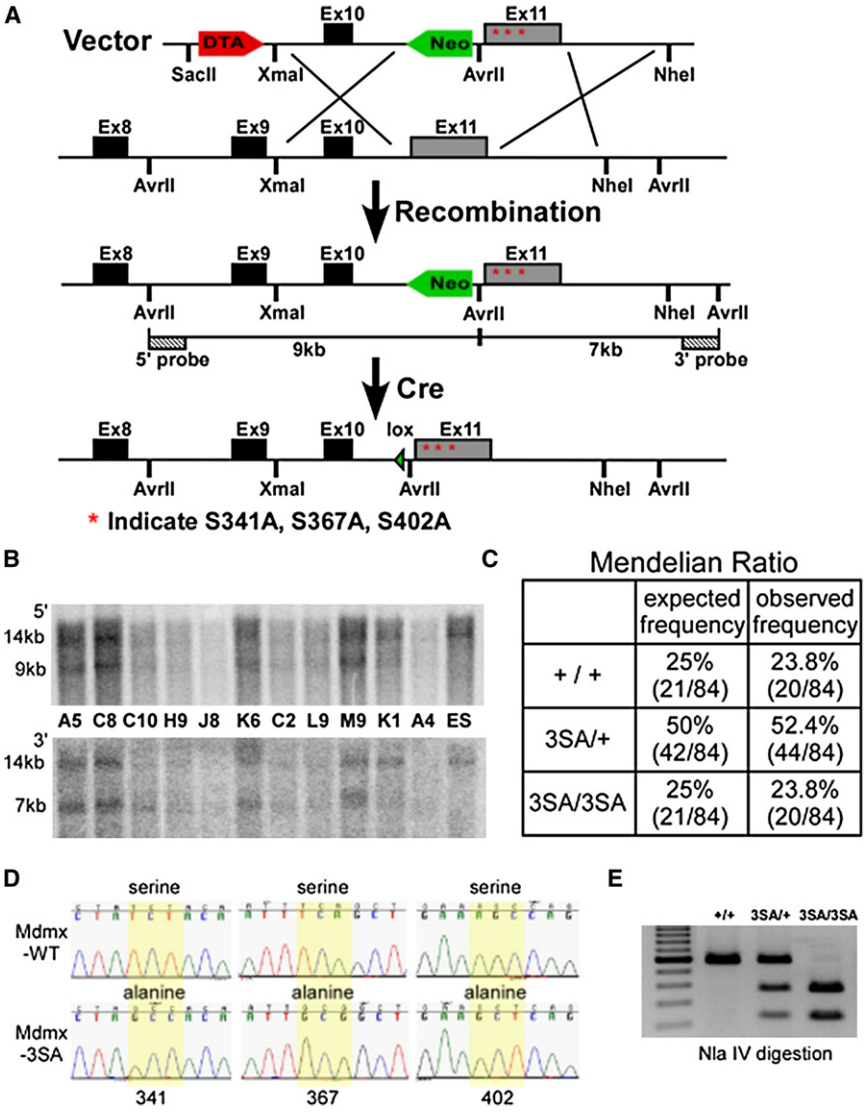

Figure 1. Generation of *Mdmx*^{3SA} Allele and Genotype Analysis of *Mdmx*^{3SA}

(A) Schematic representation of the 3′ end of the mouse *Mdmx* locus, targeting vector, and homologous recombined *Mdmx*^{3SA} allele, followed by excision of loxP-flanked Neo cassette. The targeting construct contains a DTA negative selection marker, 5′ homology region with exon 10, and a loxP-flanked Neo positive selection cassette, followed by exon 11 with *Mdmx* mutations indicated by stars and the 3′ homology region. The insertion of Neo introduces an additional AvrII site that was used for Southern analysis with the indicated external 5′ and 3′ probes. Cre expression in the male germline subsequently allows excision of Neo.

(B) Southern blot analysis of targeted ES clones. The 14 kb band represents the AvrII fragments from the wild-type allele using both 5′ and 3′ probes. The recombined allele generates a 9 kb fragment detected by the 5′ probe and a 7 kb fragment detected by the 3′ probe.

(C) The expected and observed Mendelian ratios from *Mdmx*^{3SA} heterozygote breeding.

(D) Sequences of *Mdmx* transcript expressed from *Mdmx*^{WT} and *Mdmx*^{3SA} thymus. Yellow highlight shows that the codons that encode S341, S367, and S402 of the wild-type *Mdmx* are mutated in the *Mdmx*^{3SA} allele.

(E) PCR genotype of the *Mdmx*^{3SA} mutant. PCR amplifies the region surrounding the mutations to produce a 579 bp fragment. The introduction of mutations generates an NlaIV site that results in 366 and 213 bp fragments when PCR product is digested with NlaIV.

react with any of the phospho-specific antibodies (Figures 2A and 2B), which confirms the sequencing results (Figure 1D), and further shows that one or more of the three mutated serines engender the damage-induced mobility shift of the endogenous gene product.

Mdmx^{3SA} Mutations Impair DNA-Damage-Induced Mdmx Degradation and p53 Stabilization

Previous studies in human cell lines suggest that Mdmx is a stable protein in cells not exposed to exogenous challenges. Upon DNA damage, Mdmx is modified by kinases and degraded at the proteasome (Okamoto et al., 2005; Pereg et al., 2005, 2006; Chen et al., 2005; LeBron et al., 2006). Consistent with previous studies, induction of DNA damage reduced the abundance of Mdmx^{WT} in MEFs (Figures 2C and 2D), which can be prevented by incubating cells with proteasome inhibitors (Figure S2). This indicates accelerated Mdmx^{WT} degradation following DNA damage. By contrast, the *3SA* mutations significantly reduced DNA-damage-induced Mdmx degradation (Figures 2C and 2D). No further accumulation of Mdmx^{3SA} in the presence of proteasome inhibitors was observed (Figure S2), indicating that Mdmx^{3SA} was quite resistant to DNA-damage-induced degradation. The mutations stabilize Mdmx in other cell types as well, as Mdmx^{3SA} in thymocytes was significantly more resistant to damage-induced degradation than Mdmx^{WT} after irradiation (Figure 2E). We also noticed that Mdmx^{3SA} is slightly more abundant than Mdmx^{WT} in the cells that were not exposed to exogenous DNA damage. Concomitant with a more stable Mdmx^{3SA} after DNA damage, we observed lower accumulation of p53 in Mdmx^{3SA} cells, consistent with a model in which Mdmx phosphorylation at these residues decreases its stability while increasing p53 stability (Pereg et al., 2005; Figure S2).

The Effect of Mdmx Phosphorylations on Protein Interactions

We next determined whether mutations of endogenous S341, S367, and S402 would affect 14-3-3 binding after DNA damage, as this has been suggested to contribute to Mdmx stability control (Okamoto et al., 2005; Pereg et al., 2006; LeBron et al., 2006). Cell lysates from *Mdmx*^{WT}, *Mdmx*^{3SA}, and *p53*$^{-/-}$; *Mdmx*$^{-/-}$ (2KO) MEFs were incubated with GST-14-3-3 recombinant proteins; glutathione beads were then used to isolate

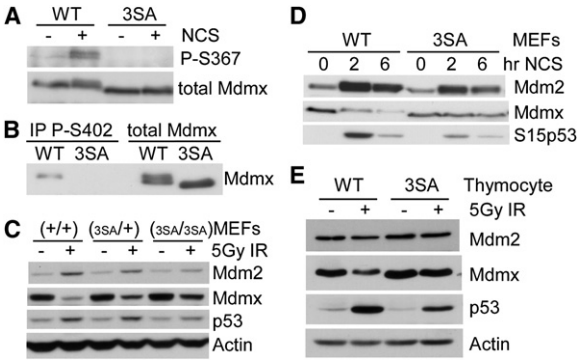

Figure 2. *Mdmx*^{3SA} Mutations Impair DNA-Damage-Induced Mdmx Degradation

(A) *Mdmx*^{WT} and *Mdmx*^{3SA} MEFs were preincubated with MG132 (10 μM) for 30 min, followed by 2 hr of NCS (200 ng/ml) incubation. Lysates were immunoprecipitated with anti-Mdmx antibody, and blotted with anti-phospho-S367 antibody.

(B) MEFs were treated as described in (A). Lysates were immunoprecipitated with anti-phospho-S402 Mdmx antibody, and blotted with anti-Mdmx antibody.

(C) MEFs were irradiated with 5 Gy of γ-irradiation. Four hours later, cells were lysed for western analysis.

(D) MEFs were treated with 200 ng/ml of NCS for 0, 2, and 6 hr. Lysates were analyzed by western blotting using antibodies against Mdm2, Mdmx, and phospho-S15 of p53.

(E) Thymocytes were irradiated with 5 Gy of γ-irradiation. Four hours later, cells were lysed for western analysis.

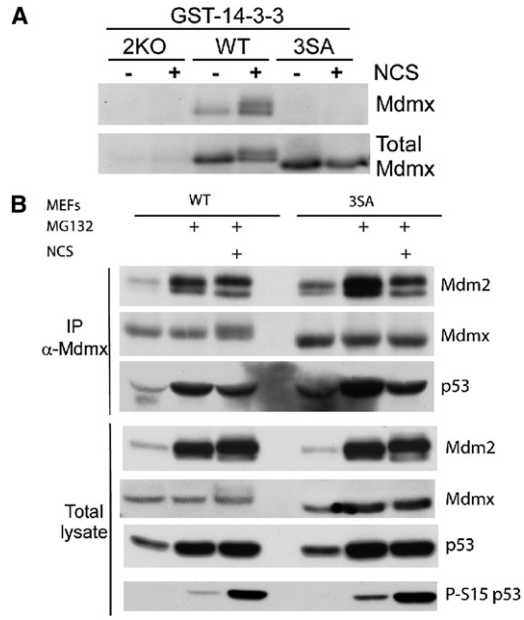

Figure 3. Analyses of Protein Interactions with Mdmx^{3SA} in Response to DNA Damage

(A) Cell lysates from *Mdmx*^{WT}, *Mdmx*^{3SA}, and 2KO (*p53*$^{-/-}$;*Mdmx*$^{-/-}$) MEFs either left untreated or treated with NCS (200 ng/ml) in the presence of MG132 (10 μM) for 2 hr were incubated with glutathione beads prebound with GST-14-3-3ε proteins. Bead-bound proteins were eluted and analyzed by western blotting.

(B) MEFs were either left untreated or treated with MG132 (10 μM) or treated with MG132 plus NCS (200 ng/ml) and lysed 2 hr after. Cell lysates were immunoprecipitated with anti-Mdmx antibody, and blotted with anti-Mdm2, anti-Mdmx, and anti-p53 antibodies. Anti-phospho-S15 of p53 antibody was used as a control for detecting the DNA damage signal induced by NCS.

proteins that bound to GST-14-3-3. Figure 3A shows that Mdmx^{WT} bound to 14-3-3 when cells were treated with NCS. In the absence of NCS, a small portion of Mdmx^{WT} was also pulled down by GST-14-3-3 (Figure 3A, lane 3, compare Mdmx to total Mdmx), which is consistent with the observation in Figure 2A that Mdmx is phosphorylated at low levels under our cell-culture conditions. On the other hand, no interaction was detected with Mdmx^{3SA}. Subcellular fractionation analyses indicated that Mdmx was predominantly cytoplasmic in untreated *Mdmx*^{WT} and *Mdmx*^{3SA} MEFs (Figure S3). Notably, the abundance of nuclear Mdmx^{3SA} was not affected by DNA damage (Figure S3).

We next investigated whether S341, S367, and S402 phosphorylations affect binding to Mdm2, as Mdmx degradation upon DNA damage is mediated by Mdm2 (Kawai et al., 2003). *Mdmx*^{WT} and *Mdmx*^{3SA} MEFs were left untreated, or exposed to NCS in the presence of proteasome inhibitors to maintain sufficient Mdmx to enable detection, and then immunoprecipitated with Mdmx-specific antibodies (Figure 3B). The data demonstrate that similar amounts of Mdm2 were coimmunoprecipitated with Mdmx^{WT} and Mdmx^{3SA} following DNA damage. Mdm2 was also coimmunoprecipitated with Mdmx^{3SA} following treatment with the topoisomerase I inhibitor etoposide (Figure S4). These data lead us to conclude that DNA-damage-induced modifications on Mdmx have little effect on its interaction with Mdm2 when both proteins are expressed at endogenous levels.

p53 Activity Is Reduced in *Mdmx*^{3SA} MEFs and Thymocytes

Mdmx antagonizes p53-induced transcription by binding the p53 transactivation domain (reviewed by Marine and Jochemsen, 2005; Toledo and Wahl, 2006). Because Mdmx degradation tracks with p53 activation (Wang et al., 2007), and Mdmx^{3SA} is more stable than Mdmx^{WT} after DNA damage, we predicted that Mdmx^{3SA} would compromise p53 activation. We therefore compared the expression of the p53 target genes *p21* and *puma* in MEFs and thymocytes. Under normal cell-culture conditions, p53 abundance in Mdmx^{WT} and Mdmx^{3SA} cells was not significantly different (Figure S9). However, we did observe a lower basal level of *p21* transcription in the Mdmx^{3SA}-expressing cells (Figure 4A). Upon DNA damage, the fold induction of *p21* was slightly lower than that in Mdmx^{WT} cells (Figure S5), but the absolute level of induced *p21* transcript was 50% of the wild-type level (Figure 4A). The reduced transcription of *p21* was manifested functionally by a reduced efficiency of DNA-damage-induced arrest in MEFs (Figures 4B and 4C).

Induction of apoptosis is a second critical function of p53, and induction of the proapoptotic gene *puma* is required for damage-induced thymic apoptosis (Erlacher et al., 2005). Consistently, we observed a lower basal level of *puma* transcription in *Mdmx*^{3SA} thymocytes and a slightly lower fold induction of *puma* after exposing mice to 5 Gy of whole-body irradiation (Figures 4A and S5). Importantly, we observed a significantly reduced abundance of *puma* transcripts in *Mdmx*^{3SA} thymocytes, and this correlated with a significant decrease in the number of *Mdmx*^{3SA} apoptotic thymocytes after ionizing radiation (Figures 4D–4F). To summarize, although the fold activation of p53-dependent

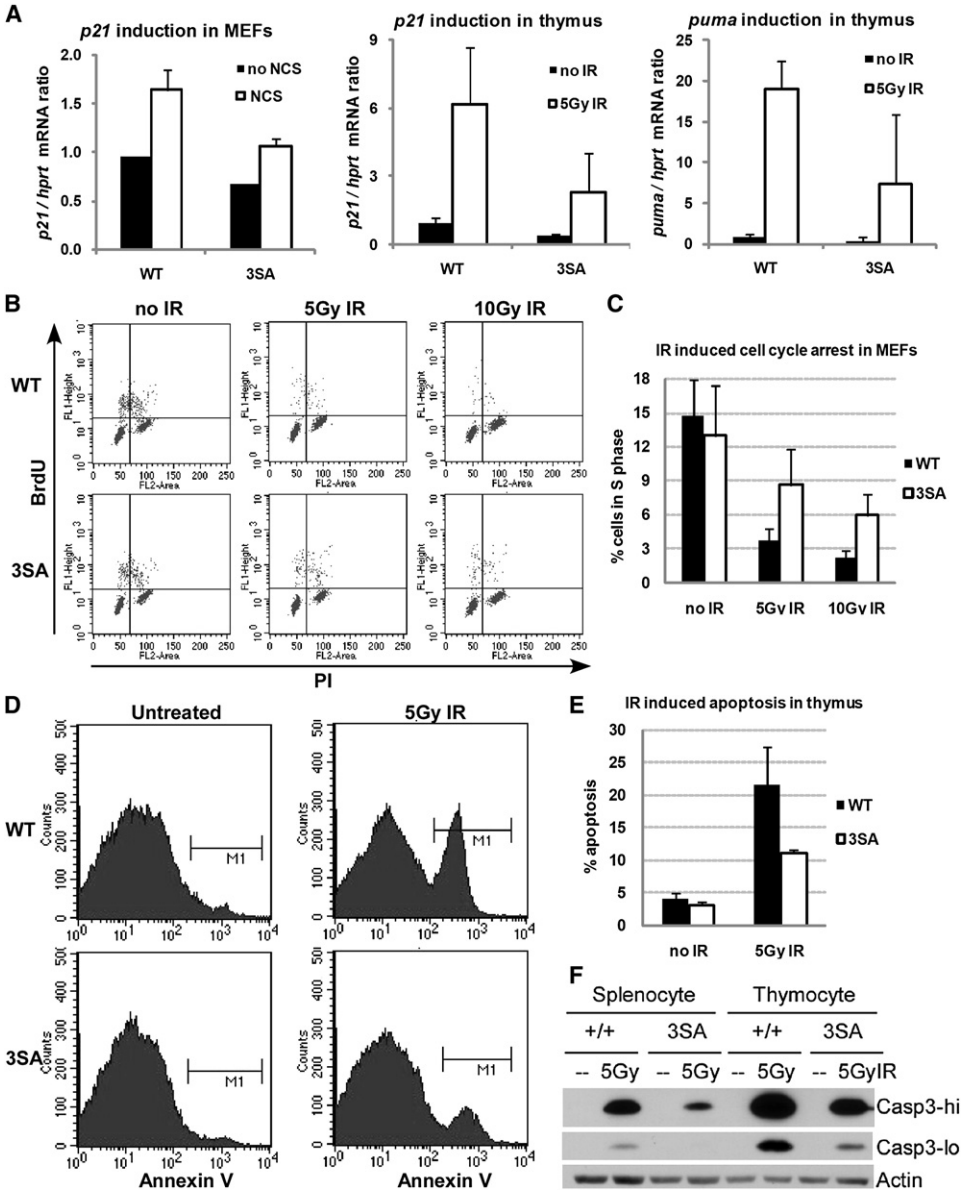

Figure 4. p53 Activity Is Reduced in *Mdmx*^{3SA} Mutant

(A) MEFs were treated with 500 ng/ml of NCS or 5-week-old mice were exposed to 5 Gy of γ-irradiation. Six hours after NCS incubation or 4 hr after irradiation, cells or thymus removed from *Mdmx*^{WT} (WT) and *Mdmx*^{3SA} (3SA) mice were lysed for RNA isolation. *p21* and *puma* gene expression was analyzed by real-time quantitative PCR. Results were normalized to *hprt* mRNA. Error bars represent ±SD from three independent experiments.

(B and C) Cell-cycle arrest analysis. MEFs were either left untreated or exposed to 5 or 10 Gy of γ-irradiation. Twenty-three hours after irradiation, 10 μM BrdU was added in the cell culture for 1 hr before FACS analysis (B). BrdU-positive cells that represent cells in S phase during BrdU incorporation are quantified in (C). Error bars represent ±SD from three independent experiments.

(D and E) Analysis of apoptosis in vivo. Mice were either left untreated or were exposed to 5 Gy of γ-irradiation. Four hours later, thymocytes were isolated from mice and stained with Annexin V-FITC for FACS analysis (D). Annexin V-positive cells that represent apoptotic cells are quantified in (E). Error bars represent ±SD from three independent experiments.

(F) Apoptosis in splenocytes and thymocytes. Mice were treated as described in (D). Splenocytes and thymocytes were isolated and analyzed for the expression of the active form of caspase-3 by western blotting with high (hi) or low exposure (lo).

transactivation is similar in *Mdmx*^{WT} and *Mdmx*^{3SA} tissues (Figure S5), the absolute mRNA level following stress is much lower in *Mdmx*^{3SA}-expressing cells. We suggest that this absolute level (rather than the fold change compared to basal expression) is what ultimately dictates the biological response.

Mdmx^{3SA} Mice Show Increased Resistance to Death Induced by Ionizing Radiation

Irradiation of mice at 10 Gy induces a p53-dependent hematopoietic syndrome characterized by severe bone marrow depletion, which results in death within 2 weeks of exposure (Komarova

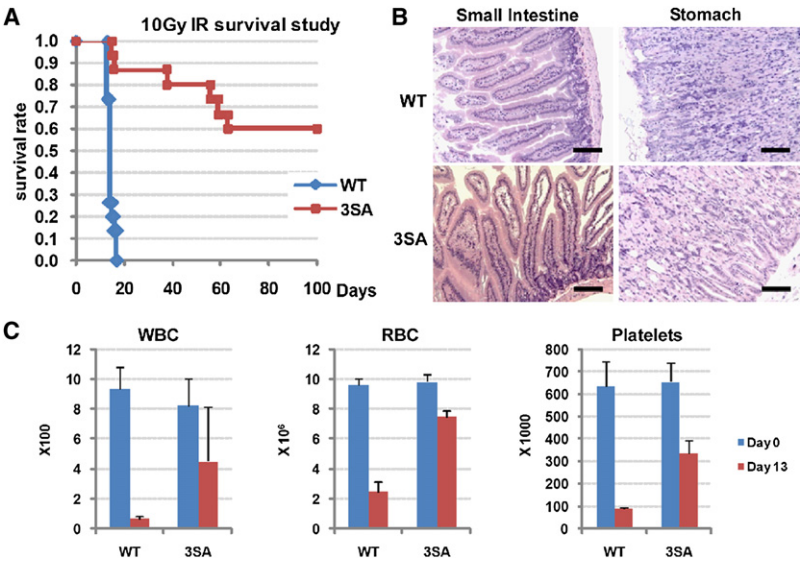

Figure 5. *Mdmx*^{3SA} Mice Are Resistant to a Lethal Dose of Ionizing Irradiation

(A) Kaplan-Meier survival curves of 15 age-matched *Mdmx*^{WT} (WT, n = 15) and *Mdmx*^{3SA} homozygote (3SA, n = 15) mice following exposure to 10 Gy of whole-body γ-irradiation.

(B) Histology of the gastrointestinal tract from *Mdmx*^{WT} and *Mdmx*^{3SA} mice showing no lesions associated with irradiation (H&E). The scale bars represent 100 μm.

(C) Complete blood count analysis of white blood cells (WBC), red blood cells (RBC), and platelets from *Mdmx*^{WT} and *Mdmx*^{3SA} mice, 13 days after 10 Gy of whole-body γ-irradiation. Error bars are ±SD from three animals.

et al., 2004). We therefore determined whether changes in Mdmx stability affect the p53 pathway and its impact on radiosensitivity in the hematopoietic compartment by comparing the effect of 10 Gy irradiation in *Mdmx*^{WT} and *Mdmx*^{3SA} mice.

As expected, a single dose of 10 Gy whole-body ionizing irradiation in *Mdmx*^{WT} 129/Sv/C57BL/6 mice resulted in death of all animals within 18 days (Figure 5A). Surprisingly, 60% of the irradiated *Mdmx*^{3SA} homozygous mice lived at least 100 days postirradiation (Figure 5A). We performed complete pathological analysis on a subset of *Mdmx*^{WT} and *Mdmx*^{3SA} mice 13 days postirradiation at the time when the first death was observed in *Mdmx*^{WT} mice. Complete blood count revealed severe leucopenia, anemia, and thrombocytopenia in *Mdmx*^{WT} mice 13 days postirradiation, whereas *Mdmx*^{3SA} mice exhibited only moderate leucopenia and thrombocytopenia and mild anemia (Figure 5C). Histopathological analysis did not show lesions in any other tissues, including the gastrointestinal tract, in either *Mdmx*^{WT} or *Mdmx*^{3SA} mice (Figure 5B). This suggests that Mdmx^{3SA} mitigates p53 activity and confers radiation resistance predominantly by affecting the hematopoietic compartment in vivo. Consistent with these data, the majority of *Mdmx*^{3SA} mice show long-term survival following irradiation at a dose that is lethal to *WT* animals. A subset of these mice exhibited moderate anemia, leucopenia, and thrombocytopenia, which allowed them to survive the acute mortality phase, but died of anemia 20–60 days postirradiation (data not shown).

Acceleration of c-Myc-Induced Lymphomagenesis in *Mdmx*^{3SA} Mice

Loss of one *Mdmx* allele enhances p53-dependent apoptosis and significantly delays the onset of c-Myc-induced lymphoma (Terzian et al., 2007). However, whether modification of Mdmx affects Myc-induced tumorigenesis is unclear. We have begun to evaluate whether Mdmx phosphorylation modulates oncogene-induced tumorigenicity using the *iMyc*$^{E\mu}$ lymphoma model. These mice develop late-onset B cell lymphomas between 6 and 21 months of age which often exhibit changes in the Arf-Mdm2-p53 tumor suppression pathway (Park et al., 2005). *Mdmx*^{3SA} mice were bred with heterozygous *iMyc*$^{E\mu}$ mice to generate *iMyc*$^{E\mu}$*;+/+* and *iMyc*$^{E\mu}$*;3SA/3SA* mice. Figure 6A shows that Mdmx^{3SA} significantly accelerated lymphomagenesis with 50% survival at 3 months of age. Tumors arising from *iMyc*$^{E\mu}$*;3SA/3SA* mice presented with severe generalized lymphadenopathy and hepatosplenomegaly (Figure 6B). Histologically, most lymphomas were diffuse, B220^{+} IgM^{+}IgD^{+} (data not shown), high-grade B cell lymphoma with intermediate-sized cells, moderate to marked anisocytosis/anisokaryosis, high mitotic index (8–16/high-power field), and abundant apoptotic cells and large macrophages containing tingible bodies producing a typical "starry-sky" effect (Figure 6C). Tumors were highly infiltrative in several tissues including liver, kidneys, lungs, meninges, eyes, and, occasionally, the gastrointestinal tract (Figure S6). Consistent with previous studies, *iMyc*$^{E\mu}$*;+/+* mice started to die by about 6 months of age with 50% survival about a year of age (Figure 6A; Park et al., 2005). On gross examination, *iMyc*$^{E\mu}$*;+/+* mice presented with marked hepatosplenomegaly and variable lymphadenopathy. Histologically, lymphomas had similar features as those observed in the *iMyc*$^{E\mu}$*;3SA/3SA* mice (data not shown).

We further investigated whether changes in Myc-induced apoptosis or cell proliferation accompanied the early onset of lymphomas in *iMyc*$^{E\mu}$*;3SA/3SA* mice. Using age-matched pretumor littermates, we observed similar increases in apoptosis in *iMyc*$^{E\mu}$*;+/+* and *iMyc*$^{E\mu}$*;3SA/3SA* splenocytes when compared to their littermates that did not contain *iMyc*$^{E\mu}$ (Figure 6D). However, we did detect significantly more *iMyc*$^{E\mu}$*;3SA/3SA* cells in the S phase (Figure 6E). Additionally, we detected phosphorylation of histone H2AX in the *iMyc*$^{E\mu}$*;3SA/3SA* splenocytes and phosphorylation of Ser15 of p53 in *iMyc*$^{E\mu}$ induced tumors, consistent with an ongoing DNA damage response and activated ATM kinase pathway in these cells (Figure S7).

Tumors arising from overexpression of c-Myc require inactivation of the p53 pathway by either *p53* mutation, loss of *Arf*, or overexpression of *Mdm2* (Eischen et al., 1999). We therefore determined whether Mdmx^{3SA} was sufficient to blunt the p53 response to c-Myc without additional disruption of the Arf-Mdm2-p53 pathway. We observed increased levels of p53 and Arf in tumors arising from *iMyc*$^{E\mu}$*;+/+* and in one *iMyc*$^{E\mu}$*;3SA/+* mouse (Figure 6F). This is consistent with the presence of one or more mutant *p53* alleles, as p53 negatively regulates Arf (Stott et al., 1998). Indeed, one out of three *iMyc*$^{E\mu}$*;+/+* tumors and one

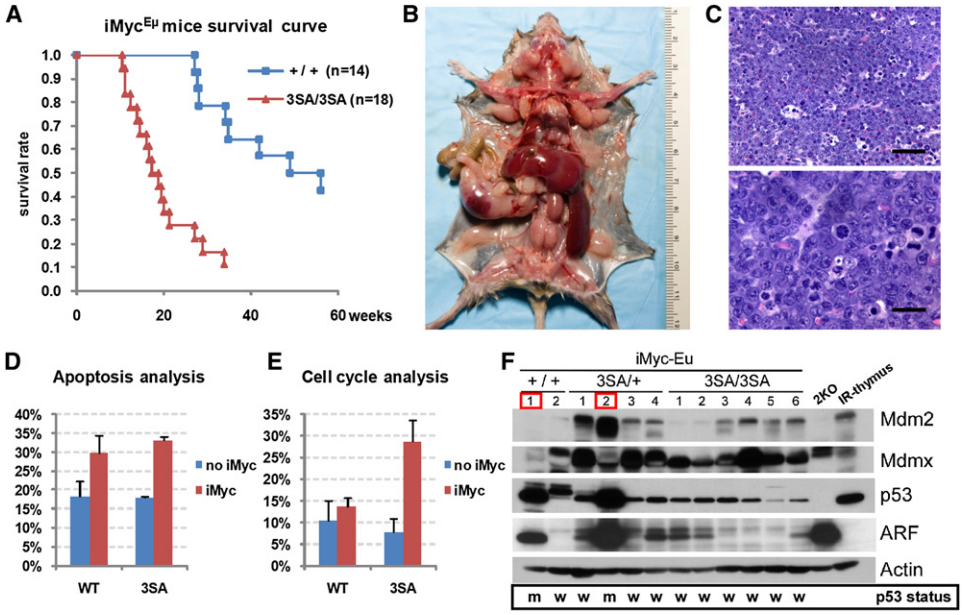

Figure 6. Myc-Induced Tumorigenesis Is Accelerated in *Mdmx*^{3SA} Mice

(A) Kaplan-Meier survival curves of *iMyc*^{Eμ}*;+/+* (n = 14) and *iMyc*^{Eμ}*;3SA/3SA* (n = 18) mice.

(B) Early-onset lymphoma in a 113-day-old *iMyc*^{Eμ}*;3SA/3SA* mouse. Dissection reveals severe enlargement of the spleen, liver, and most lymph nodes (notably the mesenteric, cervical, brachial, axillary, mediastinal, pancreatic, renal, inguinal, and lumbar nodes).

(C) High-grade B cell lymphoma in *iMyc*^{Eμ}*;3SA/3SA* mice. Upper panel: the lymph node architecture is replaced with solid sheets of intermediate-size lymphocytes admixed with apoptotic tumor cells and large macrophages containing tingible bodies producing a typical "starry-sky" effect (H&E). The scale bar represents 50 μm. Lower panel: intermediate-size lymphocytes with moderate to marked anisocytosis/anisokaryosis, high mitotic index, abnormal mitosis, and apoptotic tumor cells (H&E). The scale bar represents 20 μm.

(D) Apoptosis analysis. Splenocytes were isolated from 8-week-old littermate mice of the indicated genotypes and stained with Annexin V-FITC for FACS analysis. Annexin V-positive (i.e., apoptotic) cells were quantified. Error bars represent ±SD from three animals.

(E) Cell-cycle analysis. Eight-week-old littermate mice that contain different genotypes as indicated were intraperitoneally injected with 100 mg/kg of BrdU. Five hours later, splenocytes were isolated and stained with anti-BrdU antibody for FACS analysis. BrdU-positive cells that represent cells in S phase were quantified. Error bars represent ±SD from three animals.

(F) Levels of Mdm2, Mdmx, p53, and Arf assessed by immunoblotting in tumor extracts from *iMyc*^{Eμ}*;+/+*, *iMyc*^{Eμ}*;3SA/+*, and *iMyc*^{Eμ}*;3SA/3SA* mice. *p53*$^{-/-}$*; Mdm2*$^{-/-}$ MEFs (2KO) and thymus irradiated in vivo (IR-thymus) were used as controls. The bottom panel shows the p53 status in those tumors (w, wild-type p53; m, mutated p53). Tumor 1 from *iMyc*^{Eμ}*;+/+* and tumor 2 from *iMyc*^{Eμ}*;3SA/+* highlighted in red contain p53 mutations at R172H (CGC → CAC) and K129T (AAG → ACG), respectively (see Figure S8 for details).

out of four *iMyc*^{Eμ}*;3SA/+* tumors that were analyzed contained *p53* mutations at R172H and K129T, respectively (Figure S8). By contrast, no *p53* mutations were detected in ten *iMyc*^{Eμ}*; 3SA/3SA* tumors that were analyzed (data not shown).

DISCUSSION

Mdmx Turnover Is a Critical Component for p53 Activation In Vivo

The *Mdmx*^{3SA} mouse model presented here establishes post-translational modification of Mdmx as an important component of the damage- and oncogene-responsive mechanisms that activate p53 (Figure 7). Reducing Mdmx degradation compromised p53 transactivation of its target genes and induction of cell-cycle arrest and apoptosis. The *Mdmx*^{3SA} mice exhibit significantly reduced sensitivity of hematopoietic cells to radiation, which renders *Mdmx*^{3SA} mice extraordinarily resistant to 10 Gy of ionizing radiation (a myeloablative, lethal dose for wild-type mice). Conversely, *Mdmx*^{3SA} mice expressing the *iMyc*^{Eμ} oncogene die rapidly of widely disseminated lymphoma (see below). Thus, Mdmx regulation is involved in cellular responses to both DNA damage and some oncogenic stimuli.

Our data show that Mdmx^{3SA} is slightly more abundant than Mdmx^{WT} before DNA damage, suggesting the mutations render Mdmx more stable during homeostatic growth. We infer that a low level of stress during cell-culture conditions is responsible for this effect. This is supported by the detection of phospho-S367 in the absence of exogenous DNA damage (Figure 2A, lane 1). This "constitutive" Mdmx phosphorylation is likely responsible for degradation of Mdmx^{WT}, and thus contributes to the increase in basal levels of Mdmx^{3SA}. This may lead to the lower basal p53 activity in Mdmx^{3SA}, because Mdmx^{3SA} is now refractory to intrinsic damage-induced modification/degradation and can limit p53-dependent transactivation. Nevertheless, the functional consequence of this difference in p53 basal activity appears subtle for the following reasons: (1) Mdmx^{3SA} exhibits cell-cycle (Figure 4C) and apoptosis (Figure 4E) profiles identical to Mdmx^{WT} in the absence of exogenous DNA damage, and (2) there is no increased spontaneous tumor formation in Mdmx^{3SA} mice.

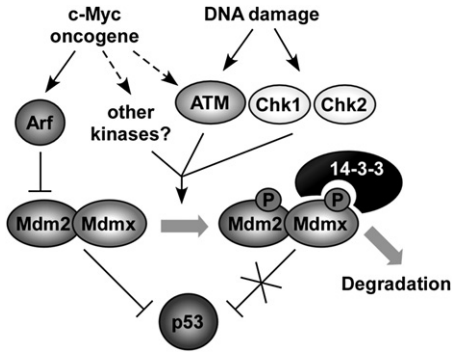

Figure 7. Mechanism for the Role of Mdmx Modification in the DNA Damage and Oncogenic Signaling Pathway

Phosphorylations of Mdmx can be initiated either by DNA damage signaling or by activated oncogenes. Phosphorylations of Mdmx modulate its interaction with other proteins, such as 14-3-3, the protein analyzed in this study. Interaction of Mdmx and 14-3-3 is required for accelerated Mdmx and Mdm2 degradation after DNA damage, probably by limiting Mdm2/Mdmx interaction with the deubiquitylase HAUSP (see text). Preferential degradation of Mdm2 and Mdmx reduces their ability to interact with and antagonize p53 function, leading to p53 activation. The *3SA* mutations introduced in this study prevent 14-3-3 interaction after DNA damage, leading to Mdmx-Mdm2 stabilization and a corresponding increased ability to degrade p53.

Interestingly, the fold induction of p53 target genes in response to DNA damage was similar between $Mdmx^{WT}$ and $Mdmx^{3SA}$ cells, although the absolute level of *p21* and *puma* transcripts was lower in $Mdmx^{3SA}$. The basal levels of p53 are similar in $Mdmx^{3SA}$ and $Mdmx^{WT}$, but damage-induced p53 levels are consistently lower in $Mdmx^{3SA}$ (Figure S9). It is important to note that the net activity of p53 results from a combination of its abundance, the interaction with and stability of its negative regulators, the effects of stress on other factors involved in p53 activation such as chromatin modifiers, etc. Note that, after stress, Mdm2 level is typically lower in the mutant due to reduced gene transcription. Thus, in $Mdmx^{3SA}$ cells after DNA damage, there is generally less Mdm2 and more Mdmx than in $Mdmx^{WT}$ cells. This results in somewhat lower p53 accumulation. The net of all these effects is the observed 2- to 3-fold decrease in activity which is apparently sufficient to prevent the biological responses required for extensive hematopoietic system apoptosis or tumor suppression. These data emphasize the importance of Mdmx regulation for setting basal and stress-induced p53 activity, and the associated biological responses.

We previously showed that p53/Mdm2 or p53/Mdmx interactions subsequent to DNA damage are readily detectable as long as proteasome inhibitors are present (Stommel and Wahl, 2004; Wang et al., 2007), implying that p53 posttranslational modifications alone are insufficient to prevent interactions with Mdm2/Mdmx. We suggest that, in addition to p53 phosphorylation, damage-induced posttranslational Mdm2/Mdmx modifications are required to enable their accelerated degradation and maximal activation of p53. Previous in vitro data showed that when Mdmx is phosphorylated, HAUSP's affinity for Mdmx is reduced, and 14-3-3's affinity is increased (Meulmeester et al., 2005; Okamoto et al., 2005; Pereg et al., 2006; LeBron et al., 2006). Consistent with this, data herein indicate that 14-3-3 binds only to phosphorylated Mdmx. Both basal and damage-induced associations of Mdmx with 14-3-3 (Figure 3) were abolished by the *3SA* mutation. This indicates that cultured cells experience sufficient stress to induce a damage response. Additionally, it may provide an explanation for the slightly elevated basal levels of $Mdmx^{3SA}$ compared to $Mdmx^{WT}$ cells, because $Mdmx^{3SA}$ is refractory to the endogenous damage signaling and can no longer bind 14-4-3. Loss of interaction between $Mdmx^{3SA}$ and 14-3-3 leads us to speculate that competition between 14-3-3 and HAUSP for Mdmx binding after DNA damage contributes to Mdmx stability control. Furthermore, we infer that 14-3-3 binding is not required for Mdmx nuclear localization per se, but that it can regulate the abundance of nuclear Mdmx following DNA damage as indicated by previous studies (LeBron et al., 2006; Pereg et al., 2006). Whether this is due to perturbed nuclear degradation of Mdmx or is a consequence of altered nucleo-cytoplasmic shuttling remains to be determined.

Mdmx Regulation Contributes to Oncogene-Mediated Activation of p53

Oncogene overexpression can activate p53 by several mechanisms (reviewed by Halazonetis et al., 2008). As one example, expressing c-Myc under the control of the Eμ immunoglobulin enhancer induces Arf expression, which antagonizes Mdm2-mediated p53 ubiquitylation, resulting in p53 activation (Zindy et al., 1998). It has been suggested that Arf does not interact with Mdmx directly (Wang et al., 2001; Li et al., 2002; Laurie et al., 2006). However, Mdmx and Mdm2 form a heterodimer and Mdmx haploinsufficiency clearly delays the onset of Myc-induced lymphomas (Terzian et al., 2007), implicating the involvement of Mdmx in the Arf-Mdm2-p53 tumor suppressor pathway. Note that most of the tumors arising from both *Eμ-Myc* mice and $iMyc^{E\mu}$ mice exhibit loss of *Arf*, *p53* mutation, or *Mdm2* overexpression (Eischen et al., 1999; Park et al., 2005). By contrast, we found no evidence of these changes in tumors arising from $iMyc^{E\mu}$*;3SA/3SA* mice. Although Mdm2 levels appear slightly elevated in some tumors arising from $iMyc^{E\mu}$*;3SA/3SA* mice compared to $iMyc^{E\mu}$*;+/+* mice, this probably reflects the lower expression of *Mdm2* in *WT* tumors that have suffered *p53* mutations. Together, these data indicate that alterations in Mdmx (either modification or stability) are sufficient to mitigate p53 function in Myc-induced lymphomagenesis.

Tumors isolated from patients often exhibit markers of double-stranded DNA damage, including phospho-ATM, phospho-Chk2, and phospho-histone H2AX (Bartkova et al., 2005), suggesting that ongoing DNA damage is a hallmark of many tumor types. Our attempts to study Mdmx phosphorylation in Myc-induced tumors by immunofluorescence were unsuccessful due to the difficulty of preserving the unstable phosphorylated form of Mdmx in vivo and current technical limitations of the available antibodies (data not shown). However, we did detect phospho-H2AX in $iMyc^{E\mu}$*;3SA/3SA* splenocytes, and phosphorylation of S15p53 in $iMyc^{E\mu}$ induced tumors, suggesting the presence of double-strand breaks and an activated ATM kinase pathway. Consistent with this inference, Myc-induced lymphomagenesis is accelerated in *ATM* deficient mice (Maclean et al., 2007). This provides a strong link between the DNA damage response and Myc-induced lymphomas. Whether the damage is triggered through Myc-induced replication stress or occurs as a consequence of lymphomagenesis itself remains

unclear. It has also been suggested that S367 of Mdmx is a target of the Akt kinase (Lopez-Pajares et al., 2008), and therefore we cannot exclude the possibility that members of other kinase families may also mediate the phosphorylations of Mdmx in response to Myc activation. Interestingly, we observed similar levels of Myc-induced apoptosis in *iMyc$^{E\mu}$;+/+* and *iMyc$^{E\mu}$;3SA/3SA* mice, whereas increased proliferation of lymphocytes was detected in *iMyc$^{E\mu}$;3SA/3SA* mice. Thus, Mdmx^{3SA} may blunt the p53 response to activated Myc, allowing more cells to enter S phase. This could explain why lymphomas develop with a shorter latency, and appear more aggressive in the *Mdmx^{3SA}* background. Indeed, in the absence of *iMyc$^{E\mu}$*, no increased spontaneous tumorigenesis was observed in *Mdmx^{3SA}* mice. This indicates that accelerated lymphomagenesis in *iMyc$^{E\mu}$;3SA/3SA* mice is via mitigation of an oncogene-induced antiproliferative response, rather than simple attenuation of basal p53 activity. In summary, our data clearly implicate Mdmx phosphorylation(s) as a determinant of oncogene-induced tumorigenesis.

Mdmx Modification in Tumorigenesis and as a Therapeutic Target

Our findings indicate that Mdmx modification is another example of the much-wielded "double-edged sword." On the one hand, phosphorylation of Mdmx appears to be critical for Mdmx degradation and tumor suppression. Thus, the function of factors controlling this process may be attenuated in cancer, and their (re)activation may be beneficial for cancer therapy. Conversely, damage-induced modification of Mdmx enhances p53-dependent radiosensitivity. In this case, *inhibition* of Mdmx phosphorylation may be a strategy to prevent cytotoxicity in normal tissues exposed to environmental or chemotherapeutic genotoxins. A precedent for this approach is the use of the p53 inhibitor pifithrin-α as a radioprotective agent in vivo (Burdelya et al., 2006). Although challenging, finding ways to promote selective Mdmx degradation in tumor versus normal cells may increase the efficacy of current p53-targeted therapies.

EXPERIMENTAL PROCEDURES

Targeting Construct

Fragments of mouse genomic *Mdmx* gene, extending from intron 9 through the 3′ UTR, were cloned into pACYC177 (New England Biolabs) using Red/ET recombination (Gene Bridges). Mutations that substitute serines 341, 367, and 402 with alanines were introduced by site-directed mutagenesis using the QuikChange kit (Stratagene). A positive selection marker, the neomycin (Neo) resistance gene, driven by the PGK promoter and flanked by loxP sites, was introduced into an AvrII site upstream of exon 11. A negative selection marker, diphtheria toxin A (DTA), driven by the PGK promoter, was inserted into the targeting vector upstream of exon 10. The exons, the intron-exon boundary, Neo, and DTA were sequenced to ensure no unexpected mutations were introduced during the cloning.

Generating and Genotyping *Mdmx^{3SA}* Mice

The targeting vector was linearized with NotI and electroporated into PrmCre 129/Sv ES cells before being selected for neomycin resistance. Homologous recombination was confirmed by PCR screening and Southern blotting with AvrII-digested genomic DNA. Southern probes were generated from PCR amplification in the regions external to the targeting vector. Four independent ES clones containing the targeted *Mdmx^{3SA}* allele were injected into C57BL/6 blastocysts, which were then implanted into pseudopregnant females. Germline transmission was confirmed by breeding chimeras with C57BL/6 mice. The offspring were PCR genotyped using a primer set (3SA-fw: 5′-AAT TTG TTC AGG TCT CAG GTT GG-3′ and 3SA-rv: 5′-CAT AAG CTA CAC GGC TTC AAG AC-3′), followed by NlaIV digestion. Heterozygous mutant mice were interbred to produce homozygous mutant mice. All animals described were on a mixed 129/Sv X C57BL/6 background.

Protein Analysis

Cells or tissues were lysed in RIPA buffer (50 mM Tris-HCl [pH 8], 150 mM NaCl, 0.1% SDS, 0.5% Na deoxycholate, 1% NP40) or in Giordano buffer (50 mM Tris-HCl [pH 7.4], 250 mM NaCl, 0.1% Triton X-100, 5 mM EDTA). Protein extracts were analyzed either by direct western blotting or by immunoprecipitation/western. Mdmx immunoprecipitations were performed with a mixture of rabbit polyclonal antibodies, p55, and p56 (Ramos et al., 2001). Blots were probed with antibodies specific for Mdm2 (4B2 [Calbiochem] and 2A10 [gift from G. Zambetti]), Mdmx (MX-82; Sigma), P-S367Mdmx and P-S402Mdmx (both gifts from Y. Shiloh), p53 (1C12; Cell Signaling Technologies), P-S15p53 (Cell Signaling Technologies), Arf (Ab80; Abcam), active caspase-3 (cleaved-caspase-3 Asp175; Cell Signaling Technologies), PARP (Santa Cruz Biotechnology), tubulin (Sigma), and actin (Sigma).

Mdmx/14-3-3 Interaction

Protein extracts made in Giordano buffer were incubated for 2 hr with glutathione beads to which bacterially produced GST-14-3-3ε was coupled. Subsequently, beads were washed four times with Giordano buffer, and bound proteins were eluted with sample buffer and analyzed by western blotting.

Quantitative PCR

RNA was isolated and subjected to real-time quantitative PCR as described previously (Krummel et al., 2005).

Flow Cytometry

For cell-cycle analysis, MEFs were irradiated with 5 or 10 Gy γ-irradiation and incubated for 23 hr, followed by 1 hr incubation with 10 μM BrdU (Sigma). For cell proliferation analysis in the *iMyc$^{E\mu}$* study, mice were intraperitoneally injected with 100 mg/ml of BrdU (Sigma). Five hours later, splenocytes were isolated. Cells were then fixed in 70% ethanol and stained with FITC anti-BrdU and propidium iodide. For the apoptosis assay, mice were exposed to 5 Gy of whole-body irradiation. Four hours later, mice were sacrificed and thymocytes or splenocytes were isolated and stained with Annexin-V-FITC (BD Biosciences) for analysis. For both cell-cycle and apoptosis analysis, the cells were sorted using a Becton Dickinson FACScan machine and data were analyzed using CellQuest Pro.

Animal Studies

All procedures were approved by the Salk Institutional Animal Care and Use Committee. For the irradiation study, age- and gender-matched mice were exposed to whole-body irradiation with a [^{60}Co]γ-irradiator. For the tumorigenicity study, *Mdmx$^{3SA/+}$* mice were bred with *iMyc$^{E\mu}$* mice to generate *iMyc$^{E\mu}$;+/+*, *iMyc$^{E\mu}$;3SA/+*, and *iMyc$^{E\mu}$;3SA/3SA* mice. Animals were observed daily for signs of morbidity and tumor development. Tumor development was monitored by palpation of the abdomen and cervical, axillary, and inguinal regions. Mice were euthanized humanely when moribund or when reaching tumor-specific endpoints. Portions of all tumors and major organs were fixed in formalin for histopathology and snap frozen for protein and RNA extraction.

SUPPLEMENTAL DATA

Supplemental Data include nine figures and can be found with this article online at http://www.cell.com/cancer-cell/supplemental/S1535-6108(09)00174-3.

ACKNOWLEDGMENTS

We thank Tomiko Velasquez and Yelena Dayn for their help with generating *Mdmx^{3SA}* mice, Dr. Inder Verma's lab for providing *iMyc$^{E\mu}$* mice, Beejal Ruparelia and Daphne Chen for mouse colony assistance and genotyping, and Rose Rodewald for technical assistance. We also wish to thank Dr. Yosef Shiloh for the phospho-Mdmx-specific antibodies and Ari Elson for GST-14-3-3 expression vectors. This work was supported by grants from the NCI (CA100845 and

CA61449 to G.M.W.) and the Cancer Center Core grant for Core Facility support (5 P30 CA014195).

Received: December 30, 2008
Revised: March 10, 2009
Accepted: May 6, 2009
Published: July 6, 2009

REFERENCES

Adams, J., Harris, A., Pinkert, C., Corcoran, L., Alexander, W., Cory, S., Palmiter, R., and Brinster, R. (1985). The c-myc oncogene driven by immunoglobulin enhancers induces lymphoid malignancy in transgenic mice. Nature *318*, 533–538.

Alitalo, K., Koskinen, P., Mäkelä, T.P., Saksela, K., Sistonen, L., and Winqvist, R. (1987). myc oncogenes: activation and amplification. Biochim. Biophys. Acta *907*, 1–32.

Bartkova, J., Horejsi, Z., Koed, K., Kramer, A., Tort, F., Zieger, K., Guldberg, P., Sehested, M., Nesland, J.M., Lukas, C., et al. (2005). DNA damage response as a candidate anti-cancer barrier in early human tumorigenesis. Nature *434*, 864–870.

Burdelya, L.G., Komarova, E.A., Hill, J.E., Browder, T., Tararova, N.D., Mavrakis, L., DiCorleto, P.E., Folkman, J., and Gudkov, A.V. (2006). Inhibition of p53 response in tumor stroma improves efficacy of anticancer treatment by increasing antiangiogenic effects of chemotherapy and radiotherapy in mice. Cancer Res. *66*, 9356–9361.

Chen, L., Gilkes, D.M., Pan, Y., Lane, W.S., and Chen, J. (2005). ATM and Chk2-dependent phosphorylation of MDMX contribute to p53 activation after DNA damage. EMBO J. *24*, 3411–3422.

Christensen, D.E., Brzovic, P.S., and Klevit, R.E. (2007). E2-BRCA1 RING interactions dictate synthesis of mono- or specific polyubiquitin chain linkages. Nat. Struct. Mol. Biol. *14*, 941–948.

de Graaf, P., Little, N.A., Ramos, Y.F., Meulmeester, E., Letteboer, S.J., and Jochemsen, A.G. (2003). Hdmx protein stability is regulated by the ubiquitin ligase activity of Mdm2. J. Biol. Chem. *278*, 38315–38324.

Eilers, M., and Eisenman, R.N. (2008). Myc's broad reach. Genes Dev. *22*, 2755–2766.

Eischen, C.M., Weber, J.D., Roussel, M.F., Sherr, C.J., and Cleveland, J.L. (1999). Disruption of the ARF-Mdm2-p53 tumor suppressor pathway in Myc-induced lymphomagenesis. Genes Dev. *13*, 2658–2669.

Eischen, C.M., Alt, J.R., and Wang, P. (2004). Loss of one allele of ARF rescues Mdm2 haploinsufficiency effects on apoptosis and lymphoma development. Oncogene *23*, 8931–8940.

Erlacher, M., Michalak, E.M., Kelly, P.N., Labi, V., Niederegger, H., Coultas, L., Adams, J.M., Strasser, A., and Villunger, A. (2005). BH3-only proteins Puma and Bim are rate-limiting for γ-radiation- and glucocorticoid-induced apoptosis of lymphoid cells in vivo. Blood *106*, 4131–4138.

Fang, S., Jensen, J.P., Ludwig, R.L., Vousden, K.H., and Weissman, A.M. (2000). Mdm2 is a RING finger-dependent ubiquitin protein ligase for itself and p53. J. Biol. Chem. *275*, 8945–8951.

Grossman, S.R., Perez, M., Kung, A.L., Joseph, M., Mansur, C., Xiao, Z.X., Kumar, S., Howley, P.M., and Livingston, D.M. (1998). p300/MDM2 complexes participate in MDM2-mediated p53 degradation. Mol. Cell *2*, 405–415.

Halazonetis, T.D., Gorgoulis, V.G., and Bartek, J. (2008). An oncogene-induced DNA damage model for cancer development. Science *319*, 1352–1355.

Jin, Y., Dai, M.S., Lu, S.Z., Xu, Y., Luo, Z., Zhao, Y., and Lu, H. (2006). 14-3-3γ binds to MDMX that is phosphorylated by UV-activated Chk1, resulting in p53 activation. EMBO J. *25*, 1207–1218.

Jones, S.N., Roe, A.E., Donehower, L.A., and Bradley, A. (1995). Rescue of embryonic lethality in Mdm2-deficient mice by absence of p53. Nature *378*, 206–208.

Kamijo, T., Weber, J.D., Zambetti, G., Zindy, F., Roussel, M.F., and Sherr, C.J. (1998). Functional and physical interactions of the ARF tumor suppressor with p53 and Mdm2. Proc. Natl. Acad. Sci. USA *95*, 8292–8297.

Kawai, H., Wiederschain, D., Kitao, H., Stuart, J., Tsai, K.K., and Yuan, Z.M. (2003). DNA damage-induced MDMX degradation is mediated by MDM2. J. Biol. Chem. *278*, 45946–45953.

Kawai, H., Lopez-Pajares, V., Kim, M.M., Wiederschain, D., and Yuan, Z.-M. (2007). RING domain-mediated interaction is a requirement for MDM2's E3 ligase activity. Cancer Res. *67*, 6026–6030.

Komarova, E.A., Kondratov, R.V., Wang, K., Christov, K., Golovkina, T.V., Goldblum, J.R., and Gudkov, A.V. (2004). Dual effect of p53 on radiation sensitivity in vivo: p53 promotes hematopoietic injury, but protects from gastrointestinal syndrome in mice. Oncogene *23*, 3265–3271.

Krummel, K.A., Lee, C.J., Toledo, F., and Wahl, G.M. (2005). The C-terminal lysines fine-tune P53 stress responses in a mouse model but are not required for stability control or transactivation. Proc. Natl. Acad. Sci. USA *102*, 10188–10193.

Laurie, N.A., Donovan, S.L., Shih, C.-S., Zhang, J., Mills, N., Fuller, C., Teunisse, A., Lam, S., Ramos, Y., Mohan, A., et al. (2006). Inactivation of the p53 pathway in retinoblastoma. Nature *444*, 61–66.

LeBron, C., Chen, L., Gilkes, D.M., and Chen, J. (2006). Regulation of MDMX nuclear import and degradation by Chk2 and 14-3-3. EMBO J. *25*, 1196–1206.

Li, C., Chen, L., and Chen, J. (2002). DNA damage induces MDMX nuclear translocation by p53-dependent and -independent mechanisms. Mol. Cell. Biol. *22*, 7562–7571.

Linke, K., Mace, P.D., Smith, C.A., Vaux, D.L., Silke, J., and Day, C.L. (2008). Structure of the MDM2/MDMX RING domain heterodimer reveals dimerization is required for their ubiquitylation *in trans*. Cell Death Differ. *15*, 841–848.

Lopez-Pajares, V., Kim, M.M., and Yuan, Z.-M. (2008). Phosphorylation of MDMX mediated by Akt leads to stabilization and induces 14-3-3 binding. J. Biol. Chem. *283*, 13707–13713.

Maclean, K.H., Keller, U.B., Rodriguez-Galindo, C., Nilsson, J.A., and Cleveland, J.L. (2003). c-Myc augments γ irradiation-induced apoptosis by suppressing Bcl-XL. Mol. Cell. Biol. *23*, 7256–7270.

Maclean, K.H., Kastan, M.B., and Cleveland, J.L. (2007). Atm deficiency affects both apoptosis and proliferation to augment Myc-induced lymphomagenesis. Mol. Cancer Res. *5*, 705–711.

Marine, J.-C., and Jochemsen, A.G. (2005). Mdmx as an essential regulator of p53 activity. Biochem. Biophys. Res. Commun. *331*, 750–760.

Marine, J.-C.W., Dyer, M.A., and Jochemsen, A.G. (2007). MDMX: from bench to bedside. J. Cell Sci. *120*, 371–378.

Martins, C.P., Brown-Swigart, L., and Evan, G.I. (2006). Modeling the therapeutic efficacy of p53 restoration in tumors. Cell *127*, 1323–1334.

Maya, R., Balass, M., Kim, S.T., Shkedy, D., Leal, J.F., Shifman, O., Moas, M., Buschmann, T., Ronai, Z., Shiloh, Y., et al. (2001). ATM-dependent phosphorylation of Mdm2 on serine 395: role in p53 activation by DNA damage. Genes Dev. *15*, 1067–1077.

Meulmeester, E., Maurice, M.M., Boutell, C., Teunisse, A.F., Ovaa, H., Abraham, T.E., Dirks, R.W., and Jochemsen, A.G. (2005). Loss of HAUSP-mediated deubiquitination contributes to DNA damage-induced destabilization of Hdmx and Hdm2. Mol. Cell *18*, 565–576.

Michael, D., and Oren, M. (2003). The p53-Mdm2 module and the ubiquitin system. Semin. Cancer Biol. *13*, 49–58.

Migliorini, D., Denchi, E.L., Danovi, D., Jochemsen, A., Capillo, M., Gobbi, A., Helin, K., Pelicci, P.G., and Marine, J.C. (2002). Mdm4 (Mdmx) regulates p53-induced growth arrest and neuronal cell death during early embryonic mouse development. Mol. Cell. Biol. *22*, 5527–5538.

Montes de Oca Luna, R., Wagner, D.S., and Lozano, G. (1995). Rescue of early embryonic lethality in mdm2-deficient mice by deletion of p53. Nature *378*, 203–206.

O'Gorman, S., Dagenais, N.A., Qian, M., and Marchuk, Y. (1997). Protamine-Cre recombinase transgenes efficiently recombine target sequences in the male germ line of mice, but not in embryonic stem cells. Proc. Natl. Acad. Sci. USA *94*, 14602–14607.

Okamoto, K., Kashima, K., Pereg, Y., Ishida, M., Yamazaki, S., Nota, A., Teunisse, A., Migliorini, D., Kitabayashi, I., Marine, J.-C., et al. (2005). DNA damage-induced phosphorylation of MdmX at serine 367 activates p53 by targeting MdmX for Mdm2-dependent degradation. Mol. Cell. Biol. *25*, 9608–9620.

Pan, Y., and Chen, J. (2003). MDM2 promotes ubiquitination and degradation of MDMX. Mol. Cell. Biol. *23*, 5113–5121.

Parant, J., Chavez-Reyes, A., Little, N.A., Yan, W., Reinke, V., Jochemsen, A.G., and Lozano, G. (2001). Rescue of embryonic lethality in Mdm4-null mice by loss of Trp53 suggests a nonoverlapping pathway with MDM2 to regulate p53. Nat. Genet. *29*, 92–95.

Park, S.S., Kim, J.S., Tessarollo, L., Owens, J.D., Peng, L., Han, S.S., Tae Chung, S., Torrey, T.A., Cheung, W.C., Polakiewicz, R.D., et al. (2005). Insertion of c-Myc into Igh induces B-cell and plasma-cell neoplasms in mice. Cancer Res. *65*, 1306–1315.

Pereg, Y., Shkedy, D., de Graaf, P., Meulmeester, E., Edelson-Averbukh, M., Salek, M., Biton, S., Teunisse, A.F., Lehmann, W.D., Jochemsen, A.G., et al. (2005). Phosphorylation of Hdmx mediates its Hdm2- and ATM-dependent degradation in response to DNA damage. Proc. Natl. Acad. Sci. USA *102*, 5056–5061.

Pereg, Y., Lam, S., Teunisse, A., Biton, S., Meulmeester, E., Mittelman, L., Buscemi, G., Okamoto, K., Taya, Y., Shiloh, Y., et al. (2006). Differential roles of ATM- and Chk2-mediated phosphorylations of Hdmx in response to DNA damage. Mol. Cell. Biol. *26*, 6819–6831.

Poyurovsky, M.V., Priest, C., Kentsis, A., Borden, K.L., Pan, Z.Q., Pavletich, N., and Prives, C. (2007). The Mdm2 RING domain C-terminus is required for supramolecular assembly and ubiquitin ligase activity. EMBO J. *26*, 90–101.

Prives, C. (1998). Signaling to p53: breaking the MDM2-p53 circuit. Cell *95*, 5–8.

Ramos, Y.F.M., Stad, R., Attema, J., Peltenburg, L.T.C., van der Eb, A.J., and Jochemsen, A.G. (2001). Aberrant expression of HDMX proteins in tumor cells correlates with wild-type p53. Cancer Res. *61*, 1839–1842.

Riley, T., Sontag, E., Chen, P., and Levine, A. (2008). Transcriptional control of human p53-regulated genes. Nat. Rev. Mol. Cell Biol. *9*, 402–412.

Schmitt, C.A., McCurrach, M.E., de Stanchina, E., Wallace-Brodeur, R.R., and Lowe, S.W. (1999). INK4a/ARF mutations accelerate lymphomagenesis and promote chemoresistance by disabling p53. Genes Dev. *13*, 2670–2677.

Shieh, S.Y., Ikeda, M., Taya, Y., and Prives, C. (1997). DNA damage-induced phosphorylation of p53 alleviates inhibition by MDM2. Cell *91*, 325–334.

Singh, R.K., Iyappan, S., and Scheffner, M. (2007). Hetero-oligomerization with MdmX rescues the ubiquitin/Nedd8 ligase activity of RING finger mutants of Mdm2. J. Biol. Chem. *282*, 10901–10907.

Stad, R., Little, N.A., Xirodimas, D.P., Frenk, R., van der Eb, A.J., Lane, D.P., Saville, M.K., and Jochemsen, A.G. (2001). Mdmx stabilizes p53 and Mdm2 via two distinct mechanisms. EMBO Rep. *2*, 1029–1034.

Stommel, J.M., and Wahl, G.M. (2004). Accelerated MDM2 auto-degradation induced by DNA-damage kinases is required for p53 activation. EMBO J. *23*, 1547–1556.

Stott, F., Bates, S., James, M., McConnell, B., Starborg, M., Brookes, S., Palmero, I., Ryan, K., Hara, E., Vousden, K., et al. (1998). The alternative product from the human CDKN2A locus, p14(ARF), participates in a regulatory feedback loop with p53 and MDM2. EMBO J. *17*, 5001–5014.

Terzian, T., Wang, Y., Van Pelt, C.S., Box, N.F., Travis, E.L., and Lozano, G. (2007). Haploinsufficiency of Mdm2 and Mdm4 in tumorigenesis and development. Mol. Cell. Biol. *27*, 5479–5485.

Toledo, F., and Wahl, G.M. (2006). Regulating the p53 pathway: in vitro hypotheses, in vivo veritas. Nat. Rev. Cancer *6*, 909–923.

Uldrijan, S., Pannekoek, W.J., and Vousden, K.H. (2007). An essential function of the extreme C-terminus of MDM2 can be provided by MDMX. EMBO J. *26*, 102–112.

Vafa, O., Wade, M., Kern, S., Beeche, M., Pandita, T.K., Hampton, G.M., and Wahl, G.M. (2002). c-Myc can induce DNA damage, increase reactive oxygen species, and mitigate p53 function: a mechanism for oncogene-induced genetic instability. Mol. Cell *9*, 1031–1044.

Varley, J.M. (2003). Germline TP53 mutations and Li-Fraumeni syndrome. Hum. Mutat. *21*, 313–320.

Vousden, K.H., and Lu, X. (2002). Live or let die: the cell's response to p53. Nat. Rev. Cancer *2*, 594–604.

Wade, M., and Wahl, G.M. (2006). c-myc, genome instability, and tumorigenesis: the devil is in the details. Curr. Top. Microbiol. Immunol. *302*, 169–203.

Wang, X., Arooz, T., Siu, W.Y., Chiu, C.H., Lau, A., Yamashita, K., and Poon, R.Y. (2001). MDM2 and MDMX can interact differently with ARF and members of the p53 family. FEBS Lett. *490*, 202–208.

Wang, Y.V., Wade, M., Wong, E., Li, Y.-C., Rodewald, L.W., and Wahl, G.M. (2007). Quantitative analyses reveal the importance of regulated Hdmx degradation for p53 activation. Proc. Natl. Acad. Sci. USA *104*, 12365–12370.

Wang, P., Lushnikova, T., Odvody, J., Greiner, T.C., Jones, S.N., and Eischen, C.M. (2008). Elevated Mdm2 expression induces chromosomal instability and confers a survival and growth advantage to B cells. Oncogene *27*, 1590–1598.

Zindy, F., Eischen, C.M., Randle, D.H., Kamijo, T., Cleveland, J.L., Sherr, C.J., and Roussel, M.F. (1998). Myc signaling via the ARF tumor suppressor regulates p53-dependent apoptosis and immortalization. Genes Dev. *12*, 2424–2433.